Natural Hazards (2021) 106:2003–2024
https://doi.org/10.1007/s11069-021-04525-y

ORIGINAL PAPER

Evaluation of parametric wind models for more accurate modeling of storm surge: a case study of Hurricane Michael

Linoj Vijayan[1] · Wenrui Huang[1] · Kai Yin[1,2] · Eren Ozguven[1] · Simone Burns[1] · Mahyar Ghorbanzadeh[1]

Received: 18 August 2020 / Accepted: 8 January 2021 / Published online: 26 January 2021

Abstract

Storm surge induced by hurricane is a major threat to the Gulf Coasts of the United States. A numerical modeling study was conducted to simulate the storm surge during Hurricane Michael, a category 5 hurricane that landed on the Florida Panhandle in 2018. A high-resolution model mesh was used in the ADCIRC hydrodynamic model to simulate storm surge and tides during the hurricane. Two parametric wind models, Holland 1980 model and Holland 2010 model, have been evaluated for their effects on the accuracy of storm surge modeling by comparing simulated and observed maximum water levels along the coast. The wind model parameters are determined by observed hurricane wind and pressure data. Results indicate that both Holland 1980 and Holland 2010 wind models produce reasonable accuracy in predicting maximum water level in Mexico Beach, with errors between 1 and 3.7%. Comparing to the observed peak water level of 4.74 m in Mexico Beach, Holland 1980 wind model with radius of 64-knot wind speed for parameter estimation results in the lowest error of 1%. For a given wind model, the wind profiles are also affected by the wind data used for parameter estimation. Away from hurricane eye wall, using radius of 64-knot wind speed for parameter estimation generally produces weaker wind than those using radius of 34-knot wind speed for parameter estimation. Comparing model simulated storm tides with 17 water marks observed along the coast, Holland 2010 wind model using radius of 34-knot wind speed for parameter estimation leads to the minimum mean absolute error. The results will provide a good reference for researchers to improve storm surge modeling. The validated model can be used to support coastal hazard mitigation planning.

Keywords Storm surge modeling · ADCIRC · Parametric wind model · Hurricane Michael

✉ Wenrui Huang
whuang@eng.famu.fsu.edu

[1] Department of Civil and Environmental Engineering, Florida A&M University-Florida State University, Tallahassee, FL 32310, USA

[2] Department of Port, Waterway and Coastal Engineering, School of Transportation, Southeast University, Nanjing 210096, China

1 Introduction

Storm surge is one of the major natural hazards, which can cause damages to coastal infrastructures and environments (Yang et al. 2014; Li et al. 2018; Bilskie and Hagen 2018; Ullman et al. 2019; Siverd et al. 2020). Because field measurement stations are often limited, numerical modeling has often been often been used to study storm surge dynamics, coastal morphology, and coastal hazard impacts. Siverd et al. (2019) assessed the temporal evolution of storm surge across coastal Louisiana. Yang et al. (2020) conducted a storm surge modeling in Salish Sea. Sun et al. (2015) conducted risk analysis of seawall overflowed by storm surge. Pan and Liu (2020) investigated storm surge impact on human projects in Yangtze Estuary. Li et al. (2015) studied storm surge overflow of levees during Hurricane Katrina. Cheng and Wang (2019) investigated beach changes induced by Hurricane Irma. Xiao et al. (2019) found that storm surge has effects on the extent of saltwater intrusion into the surficial aquifer in coastal east-central Florida. Yuan et al. (2014) found that storm surge overflow and wave overtopping affect erosion in HPTRM-Strengthened Levees. Shen et al. (2020) studied sea level rise effects on storm surge in Yangtze River Estuary. Wang and Yang (2019)'s study shows the nonlinear response of storm surge to sea-level rise. Wang et al. (2020) investigated the impacts of Hurricane Michael on coastal morphology. Results indicate that the magnitude of dune erosion was mostly controlled by the storm wave height (on top of the storm surge) and prestorm beach width. Sedimentological characteristics of storm deposits along the barrier islands, within Apalachicola Bay, and in the surrounding coastal marsh were examined using 116 sediment cores and 40 grab sediment samples Because storm surges are forced by large-scale hurricane wind and pressure, improvement of the accuracy of storm surge modeling is important for hurricane impact and hazard impact studies.

Wind fields have significant effects on the accuracy of storm surge modeling. Ding et al. (2020) integrated a process model and a parametric cyclonic wind model to simulate storm surges and waves. Yang et al. (2014)'s storm surge study was based on the wind field (H*Wind) and hurricane track data from NOAA's Hurricane Research Division (HRD) (http://www.aoml.noaa.gov/hrd). The hurricane track data included hurricane center location, central atmospheric pressure, maximum sustainable wind speed, and radius of maximum wind. Because the H*Wind field only occupies a region centered on the hurricane eye and has a radius ranging between 400 and 500 km, the wind field for the rest of the model domain outside the 500 km radius was determined based on Holland's method (Holland 1980). Pan et al. (2016) evaluated several wind models by comparing simulated wind speeds at some observed locations. However, because of the complexity and asymmetric distributions of accrual wind fields, comparison of wind speeds at limit locations is not sufficient to describe the accuracy of overall wind fields during the hurricane by parametric cyclonic wind models. Therefore, it may be more reasonable to evaluate parametric cyclonic wind models by comparing simulated and observed storm surges in the coast, especially the maximum storm surge near the landfall location. Storm surge induced by Hurricane Michael in 2018 provides a good case study for evaluating some parametric cyclonic wind models (Fig. 1).

Hurricane Michael was the first category 5 (on the Saffir–Simpson Wind Scale) hurricane to make land fall in the contiguous USA since 1992 and the first to hit the Florida Panhandle, land fall being near to Mexico Beach and Tyndal Air Force Base. The damages were primarily due to surge waves, inundation and high winds in the worst affected areas of Mexico Beach (Fig. 2). Mexico Beach is located in a sandy barrier island in the

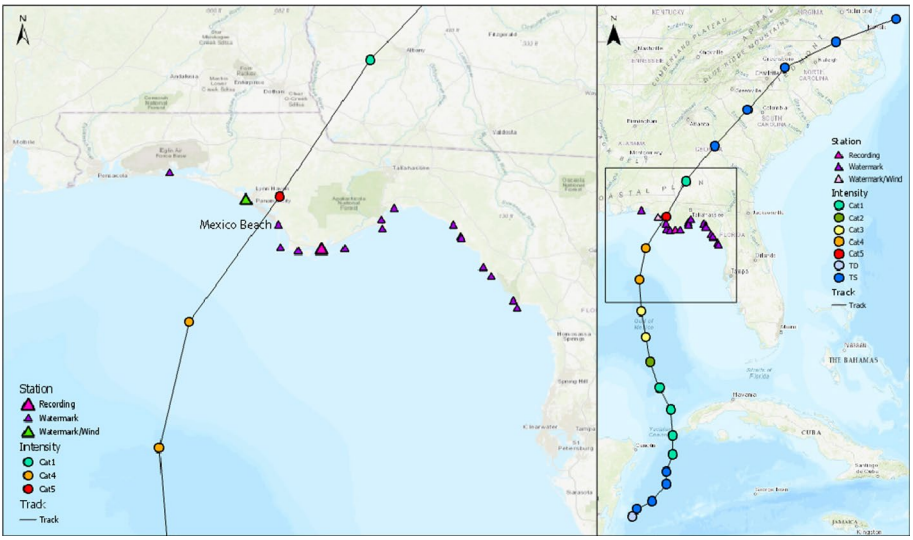

Fig. 1 Hurricane Michael track during simulation, at 6-h intervals; observed maximum water marks caused by storm tides were obtained from USGS

Fig. 2 Google photo of Mexico Beach after Hurricane Michael, showing damaged houses near beach by hurricane-induced storm surge and wind

Florida Panhandle. According to the United States Census Bureau, the city has a total area of 4.7 km^2, of which 4.6 km^2 is land. National Flood Insurance Program (NFIP) VE zone (highest risk in the 100-year floodplain) for Mexico Beach is 4.27 m. Hurricane Michael caused sand dune erosion along the beach (Wang et al. 2020). Hurricane Michael was the second major hurricane of the 2018 Atlantic hurricane season (Beven II et al. 2019). Michael caused 74 deaths including 59 in the USA and approximately $25.6 billion in total damages (Beven II et al. 2019; NCEI 2019), making it the eighth most expensive Atlantic hurricane to affect the USA. It continued on its path of destruction after landfall through states of Georgia, the Carolinas and Virginia. As a tropical disturbance in its early stages, Michael caused extreme flooding in Honduras and significant wind damage in Cuba.

The origin of Michael is attributed to a large low-pressure area in the southwestern Caribbean Sea, near the Yucatan Peninsula on October 1, 2018. It slowly became organized into a tropical depression by early hours of October 7 and became a named tropical storm later that day. While continuing in a general northward path, Michael rapidly intensified into a major hurricane of category 3 on October 9, 18:00 UTC. It attained maximum intensity of 160 mph wind gusts and a minimum central pressure of 919 mbar, at 17:30 UTC on October 10, shortly before land fall. It was then estimated to be a high end category 4 hurricane, but post season reanalysis by National Hurricane Center (NHC) showed that it was indeed a category 5 hurricane at land fall. After its landfall, Michael weakened rapidly as it made its way through the southeastern USA and reorganized into an extra tropical storm on October 12, over the Atlantic Ocean near Chesapeake Bay (Beven II et al. 2019). National Hurricane Center was closely monitoring the storm from October 7 and Florida was preparing for the impact. The State of Florida declared emergency for 35 counties by October 9. President Trump made a federal emergency disaster declaration on the same day (FDEM 2018). Four coastal counties in Florida ordered mandatory evacuation. It is estimated that 375,000 people were evacuated even though it amounted to 75% of those were ordered to evacuate (FEMA report 2020). This created some strain on roadways, especially I-10 west with major delays reported in Mobile and Pensacola, and on US highways near Panama City. Major airports in the region including Tallahassee, Pensacola, Fort Walton suspended operation from October 9th onwards. Environmental Protection Agency (EPA) assessed three Superfund sites in the Florida Panhandle, 11 in Georgia and found no releases. It also assisted Federal Emergency Management Agency (FEMA) and Florida in debris removal and management. US Army Corps of Engineers, along with Florida Department of Environmental Protection (FLDEP) and EPA restored drinking and waste water services (EPA Public affairs 2019).

United States Geological Survey (USGS) and the National Data Buoy Center (NDBC) have many wind, wave and tide levels recording stations. Most wind recording stations in the zone of influence of Michael did not have reliable recorded data during the period or the data are completely absent, owing to the unprecedented wind speed. NDBC offshore station 42,003 on October 9, 2100 UTC recorded 50-kt wind, while station 42,039 recorded only 45 kt 12 h later. Coastal station PACF1 near Panama City experienced a maximum wind of 100 kt on October 10, 18:00 UTC while another station near Apalachicola (APCF1) recorded a lower 75 kt at the same time. A number of USGS water mark locations along the Florida coast presented the maximum water levels while the station APCF1 recorded the time series of water levels above MSL. The precise location of this station is at the mouth of the Apalachicola river, indicating that the recorded water level might be influenced by the river discharge. Figure 1 shows locations of various observation stations and the path of the hurricane from October 7 UTC to October 12 UTC, 2018.

In this study, a numerical modeling study was conducted to investigate the storm surges in the Gulf of Mexico resulting from Hurricane Michael.

A high-resolution model mesh was used to resolve the Caribbean islands and Cuba as well. Two parametric cyclone wind models with inputs of wind speeds at different hurricane radii, Holland (1980) model and Holland (2010) model, are investigated to examine their effects on the accuracy of storm surge modeling. Wind and pressure data for estimating wind model parameters are obtained from HURDAT 2 (Hurricane Data version 2) archives for Hurricane Michael. Results from this study will provide a good reference for appropriate selection of a wind parametric model to adequate characterization of wind fields for more accurate storm surge simulations. It will also be helpful for emergency

management agencies and local governments to better understanding of the dynamics of storm surge for better preparing hurricane hazard mitigation plans for future hurricanes.

2 Numerical modeling methodology

2.1 Descriptions of circulation model and parametric wind model

The Advanced Circulation (ADCIRC) model developed by Luettich et al. (1992) was used to simulate the storm surge due to Hurricane Michael. ADCIRC produces reliable results while simulating coastal storm surge, as shown by number of studies around the world (Yin et al. 2017; Westerink et al. 2008; Lin et al. 2010; Fritz et al. 2010). It simulates water levels and velocities by solving the coupled equations of depth-integrated generalized wave-continuity equation (GWCE) and two-dimensional depth integrated (2DDI) momentum equations. These equations are solved by finite element method in space and finite difference method in time. The governing equations GWCE in Eq. (1) and 2DDI momentum Eq. (2) to (3) are

$$\frac{\partial \zeta}{\partial t} + \frac{\partial UH}{\partial x} + \frac{\partial VH}{\partial y} = 0 \tag{1}$$

$$\frac{\partial U}{\partial t} + U\frac{\partial U}{\partial x} + V\frac{\partial U}{\partial y} - fV = -\frac{\partial}{\partial x}\left[\frac{p_s}{\rho_0} + g(\zeta - \alpha\eta)\right] + \frac{1}{H}M_X + \frac{\tau_{SX}}{\rho_0 H} - \tau_* U \tag{2}$$

$$\frac{\partial V}{\partial t} + U\frac{\partial V}{\partial x} + V\frac{\partial V}{\partial y} + fU = -\frac{\partial}{\partial y}\left[\frac{p_s}{\rho_0} + g(\zeta - \alpha\eta)\right] + \frac{1}{H}M_Y + \frac{\tau_{SY}}{\rho_0 H} - \tau_* V \tag{3}$$

The variables in the equations are described below: t is the time; x and y are the horizontal co-ordinates, positive in the east and north directions, respectively. ζ is the free surface elevation, h is the bathymetric depth, and H is the total water column depth $= h + \zeta$; U and V are the depth-averaged horizontal velocity components in x and y directions, respectively. $f = 2\Omega \sin\phi$ is the Coriolis parameter where Ω is the angular speed of the earth and ϕ is the degrees latitude. p_s is the atmospheric pressure at the free surface, g is the acceleration due to gravity, η is the Newtonian equilibrium tide potential, α is the earth elasticity factor, and ρ_0 is the reference density of water. τ_{SX} and τ_{SY} are the applied free surface stresses in x and y directions, respectively. Bottom stress is calculated as $\tau_* = C_f\sqrt{U^2 + V^2}/H$ where C_f is the bottom friction coefficient. $M_X = E_{h2}\left[\partial^2 UH/\partial x^2 + \partial^2 UH/\partial y^2\right]$ is the depth-integrated momentum dispersion in x direction; $M_Y = E_{h2}\left[\partial^2 VH/\partial x^2 + \partial^2 VH/\partial y^2\right]$ is the depth-integrated momentum dispersion in y direction where E_{h2} is the horizontal eddy viscosity. ADCIRC is highly flexible due to its capability of solving the model equations on unstructured grids, precisely fitting irregular coastline and islands. Additionally, unstructured grids offer the convenience of a high grid resolution in the area of focus while low grid resolution in the open ocean. Various studies have also demonstrated the high skill of ADCIRC in modeling tides, storm surge, and wind-driven circulation in the Gulf of Mexico as well.

In order to simulate storm surge due to the hurricane, ADCIRC requires the pressure and wind velocity fields due to the hurricane as input meteorological forcing. Two parametric wind models by Holland (1980) and Holland et al. (2010) were investigated for their

effects of resulting symmetric wind and pressure fields on the accuracy of storm surge simulations. Holland (1980) described analytical radial profiles of pressure and wind velocity of a hurricane using two parameters, namely radius of maximum wind at any instant and a hyperbolic pressure profile parameter.

$$P(r) = P_0 + \left(P_\infty - P_0\right) exp\left[-\left(\frac{R_{\max}}{r}\right)^B\right] \tag{4}$$

$$V_G(r) = -\frac{fr}{2} + \left\{\left(\frac{fr}{2}\right)^2 + \frac{\left(P_\infty - P_0\right)B}{\rho}\left(\frac{R_{\max}}{r}\right)^B \exp\left[-\left(\frac{R_{\max}}{r}\right)^B\right]\right\}^{1/2} \tag{5}$$

where $P(r)$ is the pressure at point at a radial distance r from center of the hurricane, P_∞ is the ambient or environmental pressure (1013 mb), P_0 is the central pressure, $R_{\max}$ is the radius of maximum winds, and B is Holland's pressure profile parameter; $V_G(r)$ is the gradient balance wind velocity; ρ is the density of air; and f is the Coriolis parameter. Holland (2010) presented a revised parametric wind model. The two models differ only in the calculation of the shape parameter B as described below.

2.1.1 Shape parameter B determined by Holland (1980) wind model

$$B = \frac{V_m^2 \rho e}{100 * \left(P_\infty - P_0\right)} \tag{6}$$

where v_m is the observed maximum wind, ρ is the density of air in kg/m^3 and e is 2.718.

2.1.2 Shape parameter B determined by Holland (2010) wind model

This method uses an empirical formula involving pressure, time rate of change of center pressure, translational speed and latitude of the eye of the hurricane to calculate B.

$$B = -4.4 \times 10^{-5}\left(P_\infty - P_0\right)^2 + 0.01\left(P_\infty - P_0\right) + 0.03\frac{\partial P_0}{\partial t} - 0.014\varphi + 0.15v_t^x + 1 \tag{7}$$

where $\frac{\partial P_0}{\partial t}$ is the change in center pressure over time in hPa/hr, φ is the latitude of the center of the storm, and v_t is the translational velocity of the storm. The exponential parameter x associated with the translational velocity is calculated as $x = 0.6\left(1 - \frac{P_\infty - P_0}{215}\right)$.

In order to calculate the second parameter $R_{\max}$ in Eq. (5), we use National Oceanic and Atmospheric Administration's (NOAA) HURDAT2 data archive (Landsea and Franklin 2013). Lowest radius of 34-kt, 50-kt, and 64-kt winds among the four quadrants, along with the maximum observed wind ($V_{\max}$) on the eye wall, was used in Eq. (5), separately using the shape parameter B in Holland 1980 and Holland 2010 models. Observed $V_{\max}$ and one observed radius of known velocity were used to determine the parameter $R_{\max}$ for the radial wind profile. The best-fit wind profile in each case is obtained by minimizing the difference between observed and simulated speed $V_{\max}$ and that of wind speed at given radius (such as 34 kt, 50 kt, or 64 kt radius). Using wind data at 6-h interval during Hurricane Michael, parameters for two different parametric wind models were obtained, which can be used to produce wind fields during the hurricane. Hourly pressure and wind profiles are generated by interpolating only $V_{\max}$ and the wind radius (34 kt, 50 kt or 64 kt)

and employing the above method at each hourly time step. In short, two different methods of Holland 1980 and Holland 2010 were used to generate symmetric wind profiles, which would be used in the ADCIRC model as meteorological forcing.

2.2 Model setup

The model domain in this study was large enough to cover the path of Hurricane Michael for 5 days starting from 6 am October 7 UTC. The model runs approximately 36 h after landfall as well. The computational domain covers the entire Gulf of Mexico and Caribbean Sea as well as areas of North West Atlantic Ocean. An unstructured triangular mesh system, which fits well to irregular coastline and islands (Fig. 3), incorporating higher resolution near all coastal boundaries, was used for the computation domain. It consists of 87,367 nodes and 169,692 triangular elements with a varying resolution ranging from 25 km on the edges of the model in Atlantic Ocean to less than 1 km near the gulf coast of Florida. General Bathymetric Chart of the Oceans (https://www.gebco.net/) was used for bathymetric data and ranges from approximately 8400 m in the deep ocean to less than 1 m in coastal areas (Fig. 4). The model was forced by tidal constituents at the open ocean boundary. Principal tidal constituents were obtained from Le-provost tidal database. Simulating time step was set as 10 s. USGS river discharge data for Apalachicola River for the days of model run was also used as an input at the boundary of the Apalachicola River (https://waterdata.usgs.gov/fl/nwis/uv?site_no=02359170). Bottom friction for hydrodynamic modeling was parameterized using the spatially varying Manning coefficient values, which was ranging from 0.019 to 0.03 depending on varying bathymetry of model domain. By referring to Kerr et al. (2013) and model validations of storm surge modeling, Manning coefficient was specified as 0.019 for depth deeper than 100 m, 0.024 for depth from 7 m up to 100 m, 0.027 for depth from 3 m up to 7 m, and 0.03 for depth less than 3 m. During execution, the Manning's n values are converted to equivalent quadratic friction

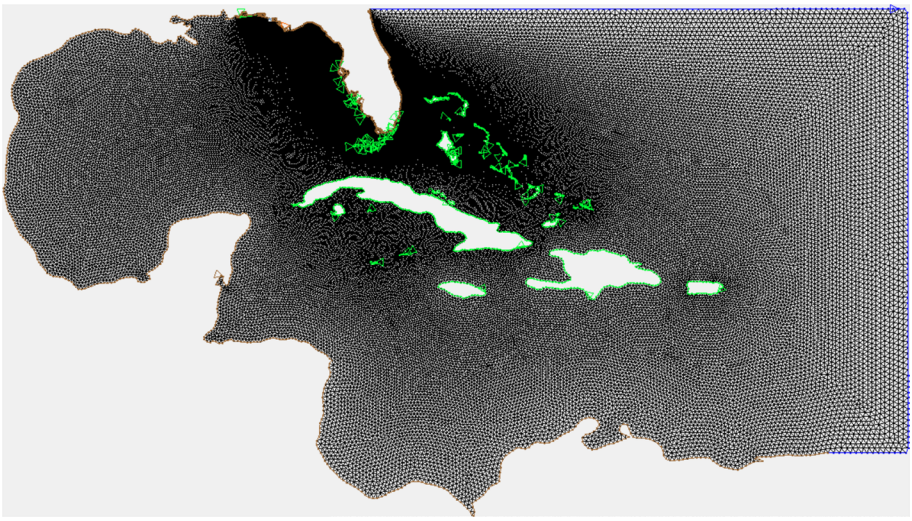

Fig. 3 Computational model mesh

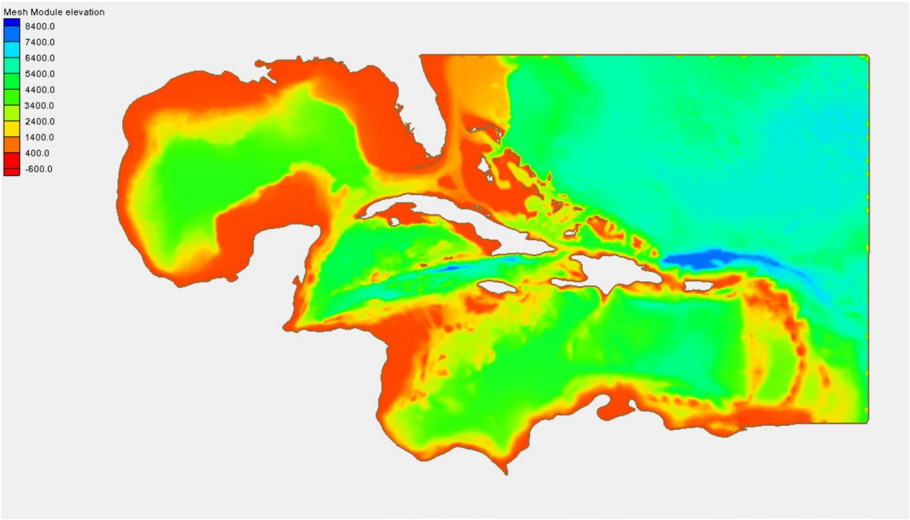

Fig. 4 Model bathymetry in meters

coefficients in the ADCIRC model before the bottom stress is calculated. The equivalent quadratic friction coefficient is calculated according to the following formula at each node at each time step:

$$C_{\mathrm{d}}(t) = \frac{gn^2}{\sqrt[3]{h + \eta(t)}} \tag{8}$$

where C_{d} is the drag coefficient with minimum value of 0.002, t is the time, g is the acceleration due to gravity, n is the Manning's n, h is the depth, and η is the water surface elevation.

3 Field observed data

HURDAT2 is a 6 hourly dataset available for all known tropical storms since 1851 (Landsea and Franklin 2013). Data for Hurricane Michael (https://www.nhc.noaa.gov/data/#hurdat) consists of its center location (longitude, latitude), translational velocity of the eye, center pressure, Coriolis parameter, observed maximum velocity of the hurricane, and observed maximum radii of 34-kt, 50-kt and 6-kt winds in the northeast, southeast, southwest and northwest (NE, SE, SW, NW) directions, at every 6-h intervals starting from 6 am UTC of October 7. Velocities are reported in knots, and the radii are reported in nautical miles. These are converted to m/s and m, respectively, for calculations in this study.

USGS high-water mark data are available for many locations in the Florida panhandle (https://stn.wim.usgs.gov/FEV). However, some of those points were well outside the model mesh while some others had unverified data, and were not used for validation. Data from 17 stations from Fort Walton Beach in the west to Cedar Key Boat Ramp in the east which were within or very close to the mesh boundary of the model were selected for validation. NDBC station at Apalachicola recorded the time series of water level during the

passage of the storm (https://www.ndbc.noaa.gov/station_history.php?station=apcf1). The water levels were measured with MLLW as vertical datum. This was converted to NAVD88 vertical datum so as to compare with the model time series output. Forcing on the open oceanic boundary of the domain consists of tidal constituents available in the Le provost tidal database available with the ADCIRC model. The Western North Atlantic, Caribbean, and Gulf of Mexico tidal database include M2, N2, S2, K2, O1, K1, and Q1 constituents (https://adcirc.org/products/adcirc-tidal-databases/) for the given time period.

4 Validations of parametric wind models

As described previously, different symmetric wind profiles were obtained using Eqs. 4 and 5, and the two parameters B and R_{max} were calculated using Holland 1980 and Holland 2010 formulae. The profiles differ if radii of different wind velocities (34 kt, 50 kt, or 64 kt) observed were used to calculate the two parameters as well because the wind profile curves have to fit data at those points. First step in validating the model input was to compare the observed and calculated V_{max}. Figure 5 shows the comparison. Both Holland 1980 and Holland 2010 formulae when used along with 50-kt and 64-kt wind radii resulted in unrealistically small R_{max}. However, to illustrate the validation method, V_{max} resulting from Holland 1980 formula with 50-kt and 64-kt wind radius each is also plotted in Fig. 5. H80_v34 in the figure represents that the method is Holland 1980 and the radius of 34-kt wind was used to determine the two parameters. Similarly, H10_v34 means that the method used was Holland 2010 and the radius of 34-kt wind was used to determine parameters. Figure 6 shows the comparison of calculated and observed center pressure.

The calculated maximum wind speed using Holland 1980 matched very well with observed maximum wind speed, no matter what the outer wind radius (34 kt, 50 kt or 64 kt) chosen. Maximum wind calculations based on Holland 2010 slightly underestimated the maximum wind especially at higher wind speeds, due to fact that the empirical formula calculating the parameter B involves temperature, latitude of the center of the hurricane, and translational speed of the hurricane. Calculated pressure had very small error

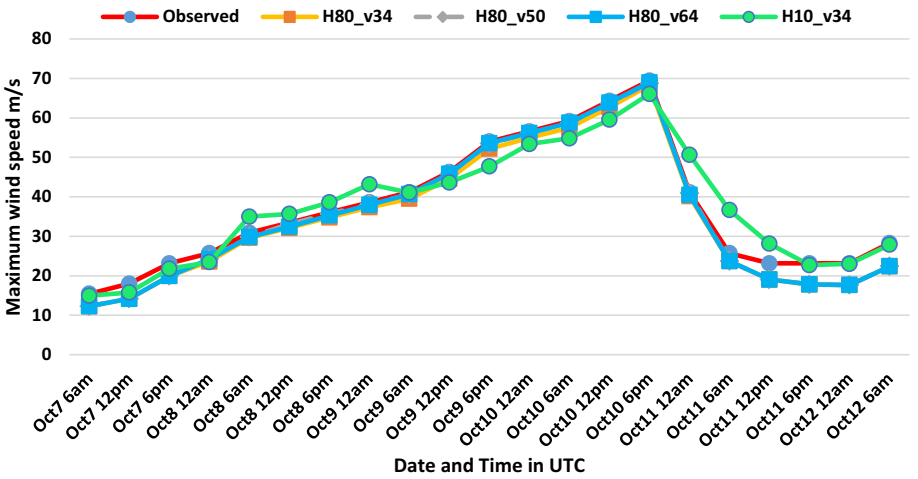

Fig. 5 Comparison of maximum wind speed computed using various methods versus observed

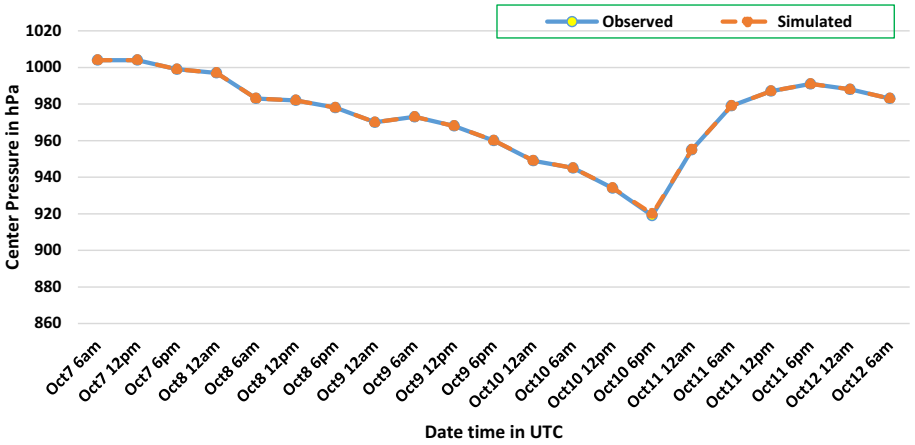

Fig. 6 Comparison of observed and calculated minimum pressure (hPa)

(4–7 hPa) with that of the observed, and the values did not change with the method (Eq. 4) as both methods use the same formula for pressure.

Wind speeds calculated by parametric models are compared to observed data at selected radius from hurricane eye. Figure 7 shows the comparison of wind speeds at the radius of 34-kt wind speeds using the two methods of Holland 1980 and Holland 2010. When Hurricane Michael was a tropical depression with winds speed less than 34 kt, available data of radii below 34-kt wind speeds were used. Results indicate that when Michael reached the hurricane strength, calculated wind speeds match well with observations at the radius of 34-knot wind observations before the hurricane made the landfall at about 17:30 UTC on October 10. Figure 8 shows the comparison of model calculated wind speeds at the radius of observed 64-kt wind speed, which also show good agreements between calculated and observed values for the period when the cyclone reached the hurricane level before landing

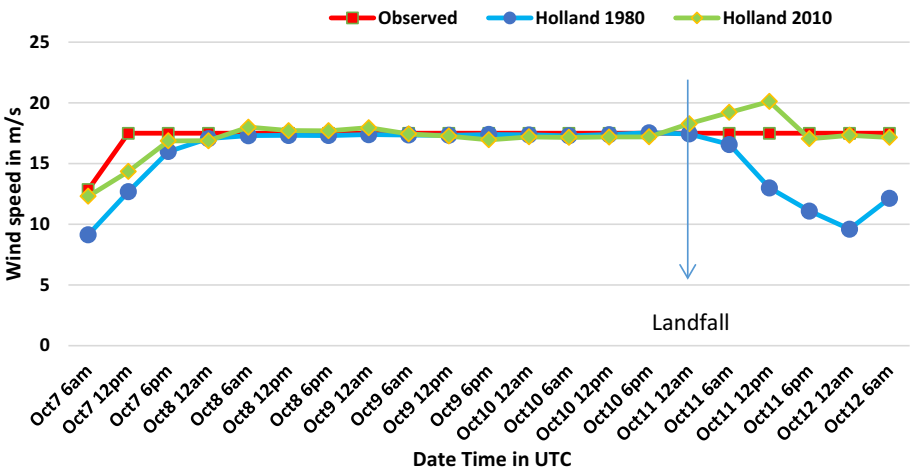

Fig. 7 Comparison of calculated wind speeds at the radius of 34 kt observed wind (17.491 m/s) by Holland 1980 and Holland 2010 methods

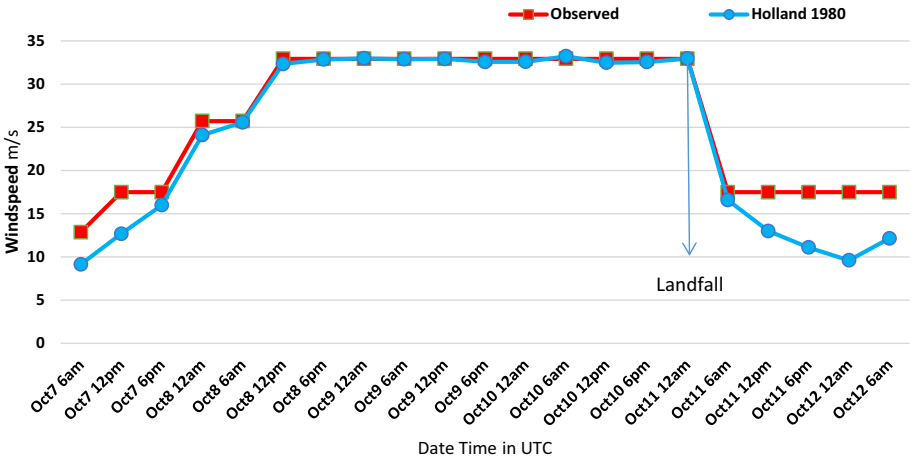

Fig. 8 Comparison of calculated wind speeds at the radius of 64 kt observed wind (32.92 m/s) computed using Holland 1980 versus observed

on Mexico Beach. A very low error in calculation resulted when the storm was a hurricane. It can also be inferred, from Figs. 6 and 7, that the parametrizations were best useful for hurricanes before landfall, as the errors increase after landfall (6 pm UTC on October 10).

Figure 9 illustrates the different characteristics in hurricane wind field when 34-kt and 64-kt wind radii was used in Holland 1980 model. The results are similar if Holland 2010 model was used. The radius of the hurricane eye wall determined by data of 64-kt wind radius is smaller than that determined by data of 34-kt wind radius. Arrows represent the profile sections for Fig. 9 where comparisons of wind profiles using the 34-kt and 64-kt wind at the indicated times are depicted. For comparison of formulae, only profiles Holland 2010 with 34-kt wind radius are shown in Fig. 10 to avoid clutter. For Holland 1980 parametrization, if the 64-kt wind radius was used in a given time step, the calculation of 34-kt wind at the observed radius would produce large errors. Based on the sensitivity study results, as use of more observation radii for the best profile would result in larger total errors, only one radius of observed wind among the 64 kt, 50 kt and 34 kt was used per time step. As a result, three separate profiles were available to force the model. These

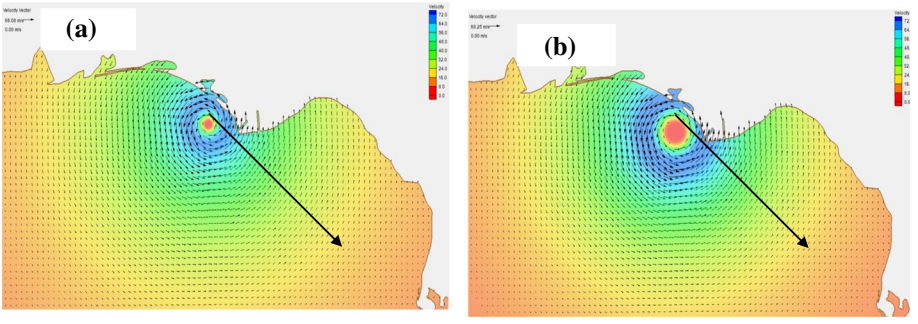

Fig. 9 **a** Symmetric wind field using Holland 1980 model with 64 kt-wind radius and **b** Holland 1980 using 34 kt-wind radius

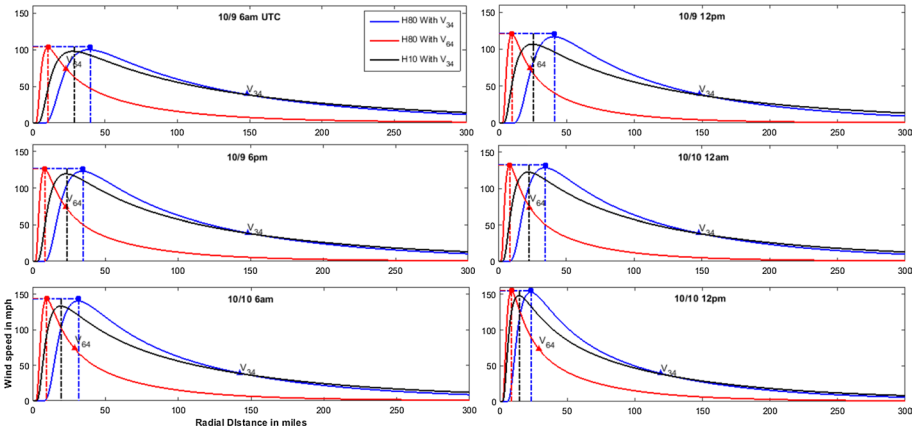

Fig. 10 Comparison of wind profiles using Holland 1980 with radii of 34-kt, 64-kt wind speed, and Holland 2010 with radius of 34-kt wind speed, at times in UTC as indicated

three different wind profiles were used to simulate storm surge separately, and their performance was evaluated by comparing the maximum storm tides with those observed at various stations in the domain. Figure 10 shows that the Holland 1980 profiles resulted in very low error in maximum velocity compared to the Holland 2010 profiles. Obviously when a larger radius of 34-kt wind was used, the result was a larger $R_{\max}$. Conversely when a smaller radius of 64 kt was used, unrealistically small $R_{\max}$ less than 10 km resulted, which was one reason why the 64 kt radii were not preferred. Another reason was that 50 kt radius and 64 kt radius resulted in very steep exponential decays at outer radii which in turn resulted in lower than observed storm surge values, especially at stations away from the eye of the storm. The profile using 50 kt radius wind was not plotted to avoid clutter. Because of these reasons, only 34 kt radii were chosen in the case of Holland 2010 parameterization.

Figure 10 also shows the limitation of the parametric wind model with wind fields controlled by model parameters determined by data from selected locations. Although the model calculated wind speed matches well with observations at the location of data selected (e.g., radius of 64 knot speed), the calculated wind speed may not match observation in another station (e.g., radius of 34 wind speed). Therefore, more accurate spatial and temporal distributions of wind field may need to be described from advanced and expensive hurricane model simulations, such as the European Centre for Medium-Range Weather Forecasts (ECMWF) Model and the Global Forecast System Model (GFS) Model by NOAA. However, due to their convenient use in applications, parametric wind models are still very popular if appropriate models are selected and validated by observations.

5 Evaluating the effects of parametric wind models on hydrodynamic modeling of storm surges

Different wind fields obtained from different parametric wind models will result in different storm surges in the coast. Effects of wind models on hydrodynamic model of storm surge were studied by comparing model simulated and observed storm tides in the coast.

Data are available from USGS and NOAA observations. Firstly, 17 USGS high-water mark stations were identified which were within the model domain (Fig. 1). Secondly, the station near Apalachicola within the model domain recorded water levels as well, which was used to validate the time series output of water levels under different wind fields obtained from different parametric wind models.

Table 1 shows the comparison of three model output maximum surge heights at these 17 recording stations with the observed values. For most locations, the maximum surge was overestimated by the Holland 1980 and under estimated by Holland 2010. At stations beyond Alligator Point, the model hurricane fields had lesser influence and so both fields recorded smaller values of maximum height than those observed. The maximum water levels due to wind field generated using Holland 2010 method had a lower mean absolute error of 0.27 m, in comparison with MAE of 0.46 m due to Holland 1980, if both methods used the 34-kt wind radius to determine the wind profile. The MAE of Holland 1980 method using 64-kt wind was 0.61 m, more than both the other methods. Figure 11 shows a bar diagram of the same comparison. It is to be noted that the stations appear on the chart from west to east. It is worth noting that at Mexico Beach, the Holland 1980 profile using 64-kt wind radius produced the lowest error, 0.05 m while the Holland 1980 using 34-kt wind radius had an error of 0.09 m. The Holland 2010 model had the maximum error in this location, 0.1775. This is attributed to the fact that the station was almost at the radius of maximum wind just before and during landfall and was directly under the forcing of maximum wind which was lower for Holland 2010 method. Due to the fact that Holland 1980 using 64-kt wind radius was the best near the landfall point, the storm surge output due to this method was also used in the validation of the time series of storm surge at Apalachicola.

The time series of surface elevations simulated by using the three different wind fields and pressure from different parametric wind models (Holland 1980 with 34 kt radii, Holland 1980 with 64 kt radii and Holland 2010 with 34 kt radii) were compared to the observations at NOAA station at Apalachicola. The time series was plotted (Fig. 12) 24 h after the model start time, allowing for model spin up. From 6 am of October 8 to 6 am of October 9 before hurricane winds affected the coastal area, water level variations were influenced mainly by diurnal tides, and hydrodynamic model simulated tidal variations reproduced well the tidal pattern as shown in the observations. The amplitude of this variation in the model was slightly over observed tidal amplitude before and after the passage of the hurricane force winds over the station. A varying river discharge (https://waterdata.usgs.gov/fl/nwis/uv?site_no=02359170) applied at the boundary of the simplified river at Apalachicola had some influence on the amplitude. The model simulated storm tides using all methods were well correlated with the observations. The Holland 2010 model was slightly better than other models correlated well and had a mean absolute error of 0.1375 m, considering only the period shown on the plot (Table 2). In comparison, the Holland 1980 with 34-kt wind and Holland 1980 with 64-kt wind had a mean absolute error of 0.1517 m and 0.1433 m, respectively.

Table 1 Comparison of errors in predicting maximum water levels at 17 different locations by using different wind models with parameters determined with different wind data

Station name	Observed (m)	H80_v34[a] (m)	H80_v64[b] (m)	H10_v34[c] (m)	Abs Error H80_v34 (m)	Abs Error H80_v64 (m)	Abs Error H10_v34 (m)
Fort Walton Beach	1.09	1.32	0.87	0.91	0.23	0.22	0.18
St Andrews Bay	1.57	2.55	2.65	1.57	0.98	1.08	0.01
Mexico Beach (hurricane landing)	4.74	4.65	4.69	4.56	0.09 (1.8%)	0.05 (1.0%)	0.18 (3.7%)
St Joseph Bay	2.41	2.92	2.96	2.48	0.51	0.55	0.07
Indian pass	2.96	3.82	3.67	3.10	0.86	0.71	0.14
Apalachicola	2.01	2.53	2.40	2.13	0.52	0.39	0.12
St George Isl	2.48	2.31	2.13	1.78	0.17	0.35	0.70
Ochlocknee bay	2.57	2.54	2.17	2.69	0.03	0.40	0.13
Alligator Pt	2.64	3.21	2.08	2.17	0.56	0.56	0.48
Goose creek bay	2.86	3.16	2.01	2.96	0.31	0.84	0.10
Big Bend Wildlife	2.52	2.28	1.93	2.14	0.24	0.59	0.38
Keaton Bch	2.35	1.91	1.64	2.13	0.44	0.71	0.22
Tide Swamp WMA	2.36	1.95	1.35	2.09	0.40	1.01	0.27
Seagrasses Pres	1.80	1.30	1.07	1.54	0.50	0.73	0.25
Horse Shoe Bch	1.89	1.12	1.01	1.52	0.77	0.88	0.37
Cedar Key	1.67	1.08	1.11	1.20	0.58	0.56	0.47
Cedar Key Boat ramp	1.67	0.97	0.99	1.13	0.70	0.68	0.54
Mean Absolute Error (MAE) (m)					0.46	0.61	0.27

[a]Holland 80_v34: storm surge output of the model with wind field generated using Holland 1980 formula with 34-kt wind radius used for parametrizing R_{max} and B

[b]Holland80_v64: Storm surge output due to Holland 1980 using 64-kt wind radius

[c]Holland10_v34: Storm surge output due to Holland 2010 using 34-kt wind radius

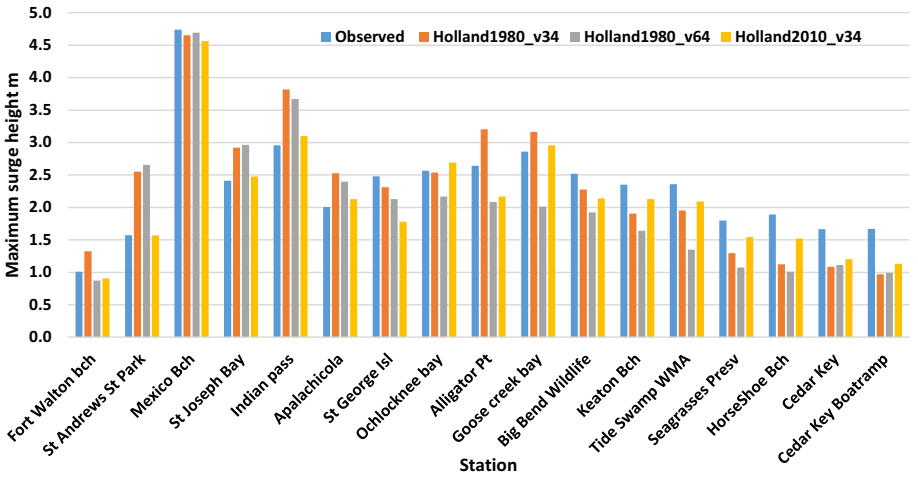

Fig. 11 Bar chart of model maximum surge at stations

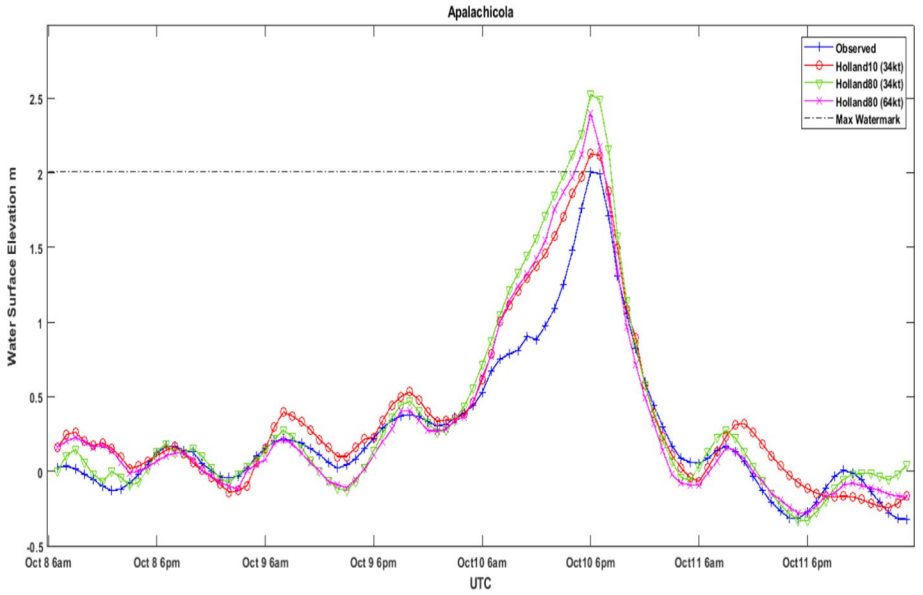

Fig. 12 Comparison of time series of model-simulated storm surge elevations with observations at NOAA station at Apalachicola station by using different wind formulae

Table 2 Comparison of error in time series of water surface elevations at Apalachicola station using different wind models

Wind model	Holland 1980 (34 kt)	Holland 1980 (64 kt)	Holland 2010 (34 kt)
RMSE (m)	0.23	0.19	0.18
Correlation coefficient	0.96	0.96	0.96
Mean absolute error (MAE) (m)	0.15	0.14	0.13

6 Comparison of wind fields under Holland 1980 and Holland 2010 wind models

As discussed above, wind profiles derived from different parametric wind models are different. In addition, controlling data points of observed radius of a given magnitude of wind speed also affect the wind profiles. One of the important parameters, the radius of maximum wind speed (R_{max}), or the radius of the hurricane wall, obtained using different wind models with different radii of maximum wind speed for parameter estimation is shown in Fig. 13.

It shows that, as the increase in hurricane strength from tropic depression on October 7 to hurricane on October 8, the radius of maximum wind gradually decreased. When the cyclone reached the hurricane strength at 6 am on October 8 until its landfall at about 6 pm October 10, the radii of maximum wind speeds were generally small. Using radius data of 64-kt wind speed for wind model parameter estimations resulted in smaller radii of maximum wind speeds than those obtained by using radius data of 34-kt wind speed for wind model parameter estimations. However, as shown in Fig. 10, the wind profiles for smaller radii of maximum wind speeds generally decreased faster than those derived from larger radii of maximum wind speeds. Referring to Table 1, the Holland 1980 with the same 64-kt wind radius profile gave very low R_{max} as well, but were used as meteorological forcing for surge simulations, resulting in the lowest error of 4 cm over a range of 4.5 m, in maximum surge value at the Mexico Beach station. It is also noted that the same method resulted in a larger overall mean absolute error (taking all 17 stations). When the Holland 1980 method using 34-kt wind radii were used, the overall RMS error was lower. Also, this method produced only a slightly larger error at Mexico Beach (8 cm over a range of 4.5 m). However,

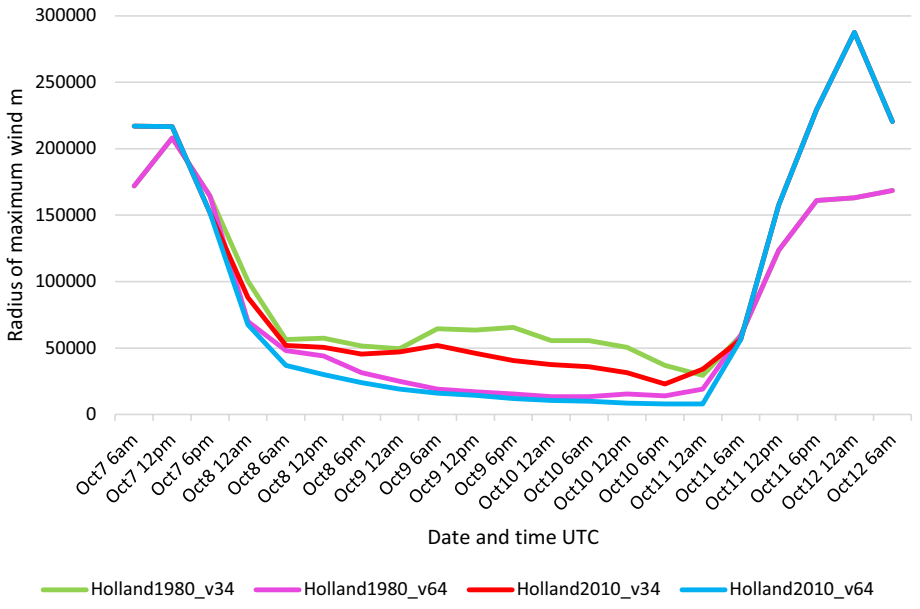

Fig. 13 Comparison of radius of maximum wind obtained by Holland 1980, Holland 2010 model with radii of 34-kt and 64-kt wind speed for parameter estimations

for the sake of brevity, only two simulations based on Holland 1980 using 64-kt wind radii and Holland 2010 using 34-kt wind radii are discussed and compared in detail below.

Spatial distributions of wind field are shown in Fig. 14 at 12-h intervals from 6 pm October 9 UTC to 5 pm October 10 UTC, time of land fall. The wind fields at any given instant in the model using 34-kt wind radius (here Holland 2010) have a larger eye wall compared to the model using 64-kt wind radius as shown by the red region at the center of the wind field. Higher wind velocities identified as blue rings close to the eye of the hurricane were also larger in the Holland 2010 model. The sizes of the wind fields indicated by the yellow rings are significantly larger in the Holland 2010 model with the radius of 34 kt for parameter estimation, which results in relative higher storm surge along coast

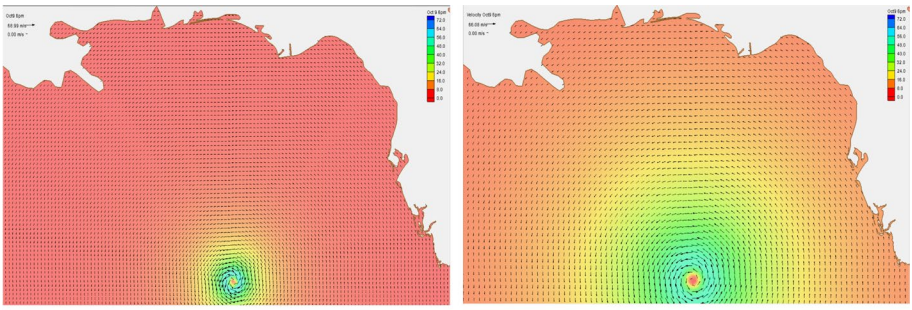

(a) Wind fields due to Holland 1980 (left) and Holland 2010 on **Oct 9, 6pm UTC**

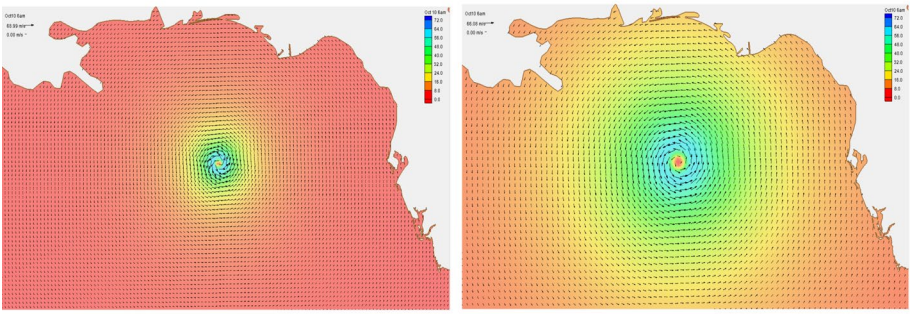

(b) Wind fields due to Holland 1980 (left) and Holland 2010 on Oct 10, 6 am UTC

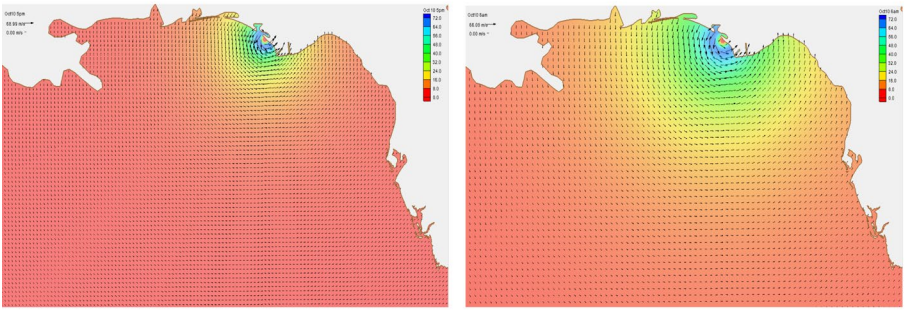

(c) Wind fields due to Holland 1980 (left) and Holland 2010 at Oct 10 5pm UTC

Fig. 14 Comparison of wind fields by using Holland 1980 on the left column and Holland 2010 on the right column

away from hurricane landing location. However, the maximum wind speed is slightly higher in the Holland 1980 model with radius of 64-kt wind speed for parameter estimation, which results in higher peak storm surge in the location of hurricane landing as shown in Table 1. For Holland 1980 wind model, however, the exponential decay of velocities radially outward (determined by the parameter B) from the eye wall of the hurricane is faster so that the wind speeds in the regions outside the hurricane eye wall are generally weaker than derived from Holland 2010 model. The maximum velocity obtained from the Holland 1980 model approximately at landfall is slightly higher (69 m/s) than the maximum velocity obtained from Holland 2010 model (66 m/s). In short, the Holland 1980 model resulted in slightly faster winds at the center than the Holland 2010 model, but wind speeds from Holland 1980 model decay faster as distance increasing from the hurricane eye wall. Although both models are reasonably validated by observed wind data at selected locations, validations of winds at selected locations for the simple parametric wind model are unable to accurately describe the entire complex wind fields. Therefore, comparison of model simulated and observed storm surges can be used as another validation for examining whether wind fields are reasonably described or not.

7 Comparison of spatial distributions of storm tides resulting from Holland 1980 and 2010 wind models

The water surface elevations, or the storm tides as the combination of storm surge and tides, from two different wind models were compared as described in Fig. 15a–c. The time stamps are, respectively, the same as the wind fields as shown in Fig. 14a–c. Left panes represent model output of Holland 1980 using 64-kt wind radii and the right ones that of Holland 2010 using 34-kt wind radii. In the early stages, the difference between the two model outputs, especially near the coastlines, was very small, as the major influence on the water surface elevation is the diurnal tides in the gulf coast. In Fig. 15a, the difference in output could be directly seen as a higher water surface elevation around the eye of the hurricane, Holland 2010 model having a larger size than that of Holland 1980 owing to the larger hurricane eye. This higher elevation region beneath the eye wall was visible in subsequent plots as well (Fig. 15b). The coasts were not experiencing surge due to hurricane yet. The coastal and near shore areas were showing marked difference in elevation close to land fall, as noticed in Fig. 15c, where Holland 1980 showed a slightly higher elevation than Holland 2010 very close to the land fall region. However, storm surges resulting from Holland 2010 extended to a large area of coastal line. The effect of a larger hurricane forced wind field is evident at landfall. At points away from the eye wall, higher storm surges resulted when Holland 2010 model was used. The coast to the left of the hurricane track experienced negative surge as indicated in both the models. This was due to the counter clockwise rotation of the hurricane, wind would blow out to the ocean, pushing water away from the shore. After the land fall, the hurricane intensity decreased drastically, but was fast moving over land, and the waves on the shore were mainly due to the tidal forcing. Additionally, the model winds were erratic after the landfall as described in the validation section and were not used in this section.

Figure 16 shows the time series of water surface elevations at Mexico Beach where hurricane Michael landed on. There were no recording stations for water levels in Mexico Beach. A highest-water mark obtained by USGS after the hurricane was available which recorded roughly 4.7 m of water level, above the FEMA's 100-year flood risk

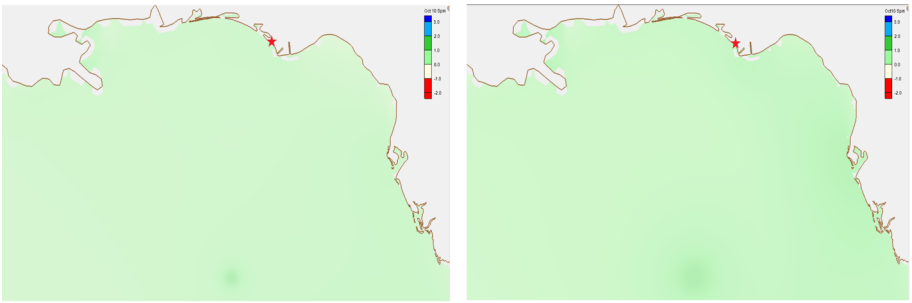

(a) Water surface elevation using Holland 1980 (left) and Holland 2010 at Oct 9, 6pm UTC

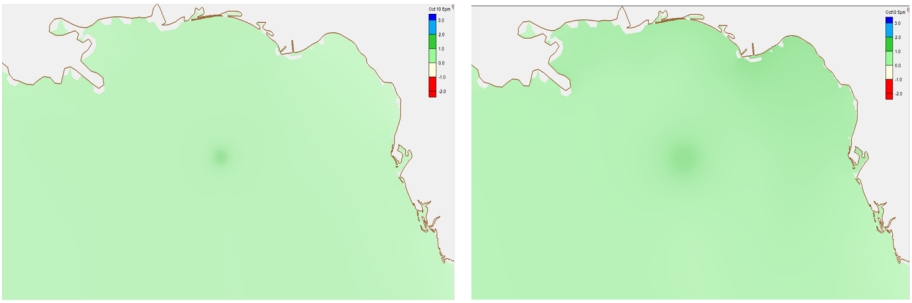

(b) Water surface elevation using Holland 1980(left) and Holland 2010 at Oct 10, 6am UTC

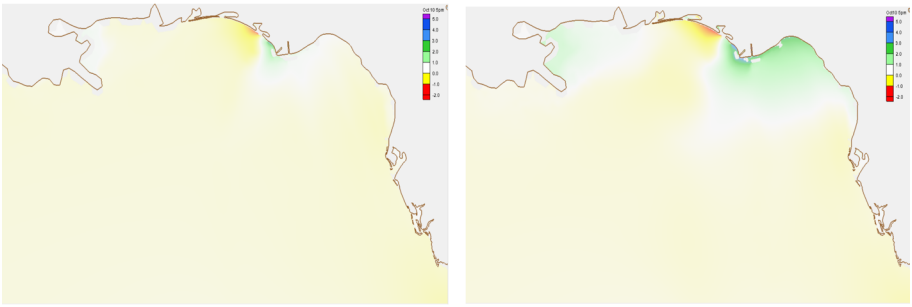

(c) Water surface elevation using Holland 1980 (left) and Holland 2010 at Oct 10, 5pm UTC

Fig. 15 Comparison of storm surge modeled by using Holland 1980 on the left column and Holland 2010 on the right column. Location of Mexico Beach is indicated with a star mark in **a**

elevation of 4.27 m. From above discussion as shown in Table 1, comparing to observed maximum water mark, model simulated maximum water level is satisfactory, with 1% error for Holland 1980 wind model and 3.7% error from Holland 2010 wind model. The difference of maximum elevation between Holland 1980 and Holland 2010 models was not significant at this location in Mexico Beach. But it can be seen that the Holland 1980 model showed a slightly higher elevation close to landfall owing to its slightly faster maximum wind compared to the Holland 2010 model and the proximity of the location to the eye wall. However, as detailed in the above discussion, different distributions of wind fields affect the storm surges along the coast (Fig. 15), which shows more difference in other observation stations as shown in Table 1 and Fig. 11.

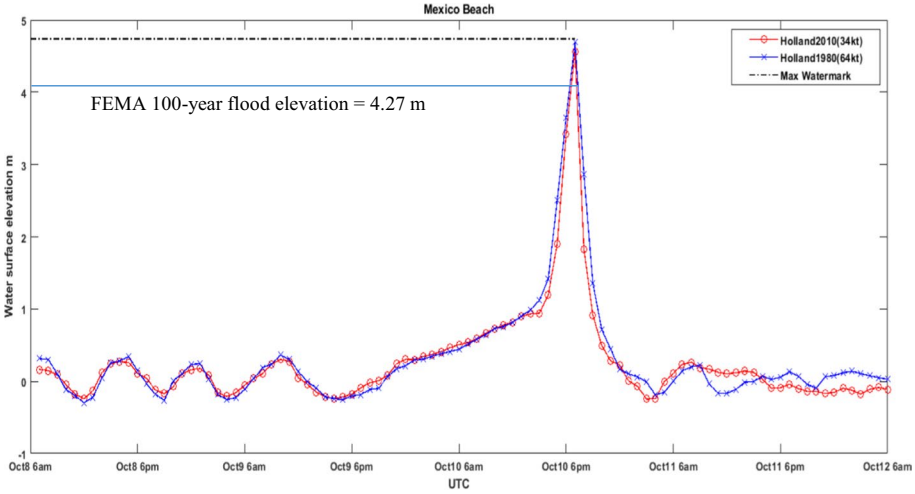

Fig. 16 Comparison of time series of storm surge at Mexico Beach using two model wind fields, Holland 1980_64knot (minimum error at Mexico Beach station for peak surge) and Holland 2010_34knot (minimum mean error over 17 stations)

An important factor to consider while prescribing the wind field is the radius of observed wind velocity that is used for wind model parameter estimation. Using the larger radius wind data for parameter estimation results in stronger wind fields away from the hurricane eye wall, which will produce higher storm surges for a larger coastal region. Final selection of an appropriate parametric wind model will depend on the comparison between model simulated and observed storm tides among stations along the coast. For the case study of Hurricane Michael, the Holland 2010 wind model using the radius of 34-knot wind speed for parameter estimation would be recommended because it results in an acceptable error of 3.7% in maximum water level in Mexico Beach and the minimum mean absolute error over 17 stations. The storm surge hydrograph reproduced from this study will be helpful for researchers to investigate temporal inundation process in Mexico Beach, which can be used to study storm surge impacts on coastal infrastructures and beach erosion, and prepare hurricane resilience plans. For potential hurricanes in north west Florida coast, the model can be used to predict the storm surges so that emergency responses actions can be taken to reduce hurricane losses. Storm surge predictions can also be used predict potential coastal flooding on roadways so that evacuation traffic can avoid flooded roads.

8 Conclusions

Adequate estimation of wind field has significant effects on the accuracy of storm surge modeling. Two symmetric wind models, Holland 1980 and Holland 2010 models, have been evaluated in the case study of storm surge modeling during Hurricane Michael, a category 5 hurricane landed on Mexico Beach in Florida coast. A circulation model (ADCIRC) was setup to simulate storm surge and tides. The hydrodynamic model was forced with tidal constituents at the ocean boundary and wind forcing on the surface. Results indicate that both Holland 1980 and Holland 2010 wind model produced reasonable accuracy in predicting maximum water level in Mexico Beach, with error between 1

and 3.7%. The peak storm surge is above the FEME's 100-year flood risk elevation. Comparing to the observed peak water level of 4.74 m in Mexico Beach, Holland 1980 wind model with radius of 64-knot wind speed for parameter estimation results in the lowest error of 1%. However, wind fields away from hurricane wall using radius of 64-knot wind speed for parameter estimation are generally weaker than those using radius of 34-knot wind speed. As the results, comparing to 17 water mark observations along the coast and hourly measurements at NOAA gage in Apalachicola, Holland 2010 wind model using radius of 34-knot wind speed for parameter estimation shows the minimum average error and root-mean-square error, indicating that Holland 2010 wind model more reasonably describes the wind field outside of the hurricane eye wall. The spatial distribution of maximum water levels along the coast shows that the coastline to the west of Mexico City of hurricane landing was less affected due to the negative storm surge as the hurricane force wind was away from the land to the ocean. The effects of hurricane on the coastal areas east of Mexico Beach were fortunately reduced by a number of barrier islands. While the results of wind model evaluations will provide a valuable reference for the improvement of storm surge modeling, the storm surge model validated for Hurricane Michael can be used to support hurricane response and mitigation planning in Florida.

Acknowledgements This study was supported by National Science Foundation Award #1832068. Mr. Kai Yin conducted preliminary model development as a visiting student in FAMU-FSU College of Engineering sponsored by China Scholarship Council. The authors appreciate Rick Luettich's help for providing the ADCIRC code to support our study.

References

Beven II JL, Berg R, Hagan A (2019). Tropical cyclone report: Hurricane Michael (AL 142018) 7–11 October 2018. National Hurricane Center

Bilskie MV, Hagen SC (2018) Defining flood zone transitions in low-gradient coastal region. Geophys Res Lett 45(6):2761–2770

Cheng J, Wang P (2019) Unusual beach changes induced by Hurricane Irma with a negative storm surge and post storm recovery. J Coastal Res 35(6):1185–1199

Ding Y, Ding T, Rusdin A, Zhang Y, Jia Y (2020) Simulation and prediction of storm surges and waves using a fully-integrated process model and a parametric cyclonic wind model. J Geophys Res Oceans. https://doi.org/10.1029/2019JC015793

FEMA Mitigation Assessment Team Report (2020) Hurricane Michael in Florida: building performance observations, recommendations and technical guidance

Florida Division of Emergency Management (2018) https://www.floridadisaster.org/news-media/news/20181009-gov.-scott-federal-pre-landfall-emergency-declaration-signed-by-the-president/

Fritz HM, Blount CD, Albusaidi FB, Al-Harthy AHM (2010) Cyclone Gonu storm surge in Oman. Estuar Coast Shelf Sci 86:102–106

Holland GJ (1980) An analytic model of the wind and pressure profiles in hurricanes. Mon Weather Rev 108:1212–1218

Holland GJ, Belanger JI, Fritz A (2010) A revised model for radial profiles of hurricane winds. Mon Weather Rev 138:4393–4401

Kerr PC, Martyr RC, Donahue AS, Hope ME, Westerink JJ, Luettich RA, Kennedy AB, Dietrich JC, Dawson C, Westerink HJ (2013) U.S. IOOS coastal and ocean modeling testbed: evaluation of tide, wave, and hurricane surge response sensitivities to mesh resolution and friction in the Gulf of Mexico. J Geophys Res Oceans 118:4633–4661. https://doi.org/10.1002/jgrc.20305

Landsea CW, Franklin JL (2013) Atlantic hurricane database uncertainty and presentation of a new database format. Mon Weather Rev 141:3576–3592

Li L, Yuan S, Amini F, Tang H (2015) Numerical study of combined wave overtopping and storm surge overflow of HPTRM strengthened levee. Ocean Eng 97:1–11

Li L, Yang J, Lin C-Y, Chua CT, Wang Y, Zhao K, Wu Y-T, Liu PL-F, Switzer AD, Mok KM, Wang P, Peng D (2018) Field survey of Typhoon Hato (2017) and a comparison with storm surge modeling in Macau. Nat Hazards Earth Syst Sci 18:3167–3178

Lin N, Emanuel KA, Smith JA, Vanmarcke E (2010) Risk assessment of hurricane storm surge for New York City. J Geophys Res Atmos. https://doi.org/10.1029/2009JD013630
Luettich RA Jr, Westerink JJ, Scheffner NW (1992) ADCIRC: an advanced three-dimensional circulation model for shelves, coasts, and estuaries. Report 1. Theory and methodology of adcirc-2ddi and adcirc-3dl; Dredging Research Program Technical Report DRP-92-6; US Army Corps of Engineers
National Centers for Environmental Information (NCEI) (2019) Assessing the U.S. climate in 2018
Pan Y, Chen Y, Li J, Ding X (2016) Improvement of wind field hindcasts for tropical cyclones. Water Sci Eng 9(1):58–66
Pan ZH, Liu H (2019) Extreme storm surge induced coastal inundation in Yangtze Estuary regions. J Hydrodyn 31(6):1127–1138. https://doi.org/10.1007/s42241-019-0086-1
Pan Z, Liu H (2020) Impact of human projects on storm surge in the Yangtze Estuary. Ocean Eng 196:106792
Shen Y, Deng G, Xu Z, Tang J (2020) Effects of sea level rise on storm surge and waves within the Yangtze River Estuary. Front Earth Sci 13:303–316. https://doi.org/10.1007/s11707-018-0746-4
Siverd CG, Hagen SC, Bilskie MV, Braud DH, Gao S, Peele RH, Twilley RR (2019) Assessment of the temporal evolution of storm surge across coastal Louisiana. Coast Eng 150:59–78
Siverd CG, Hagen SC, Bilskie MV, Braud DH, Twilley RR (2020) Quantifying storm surge and risk reduction costs: a case study for Lafitte, Louisiana. Clim Change. https://doi.org/10.1007/s10584-019-02636-x
Sun Z, Huang S, Nie H, Jiao J, Huang S, Zhu L, Xu D (2015) Risk analysis of seawall overflowed by storm surge during super typhoon. Ocean Eng 107:178–185
Ullman DS, Ginis I, Huang W, Nowakowski C, Chen X, Stempel P (2019) Assessing the multiple impacts of extreme hurricanes in Southern New England, USA. Geosciences 9(6):265
United States Environmental Protection Agency, Public Affairs (2019) https://response.epa.gov/site/site_profile.aspx?site_id=13982
Wang P, Adam JD, Cheng J, Vallée M (2020) Morphological and sedimentological impacts of Hurricane Michael along the northwest Florida coast. J Coastal Res 36(5):932–950
Wang T, Yang Z (2019) The nonlinear response of storm surge to sea-level rise: a modeling approach. J Coastal Res 35(2):287–294
Westerink JJ, Luettich RA, Feyen JC, Atkinson JH, Dawson C, Roberts HJ, Powell MD, Dunion JP, Kubatko EJ, Pourtaheri HA (2008) Basin-to channel-scale unstructured grid hurricane storm surge model applied to Southern Louisiana. Mon Weather Rev 136:833–864
Xiao H, Wang D, Medeiros SC, Bilskie MV, Hagen SC, Hall CR (2019) Exploration of the effects of storm surge on the extent of saltwater intrusion into the surficial aquifer in coastal east-central Florida (USA). Sci Total Environ 648:1002–1017. https://doi.org/10.1016/j.scitotenv.2018.08.199
Yang Z, Wang T, Castrucci L, Miller I (2020) Modeling assessment of storm surge in the Salish Sea. Estuar Coast Shelf Sci 238:106552
Yang Z, Wang T, Leung R, Hibbard K, Janetos T, Kraucunas I, Rice J, Preston B, Wilbanks T (2014) A modeling study of coastal inundation induced by storm surge, sea-level rise, and subsidence in the Gulf of Mexico. Nat Hazards 71:1771–1794
Yin K, Xu S, Huang W, Xie Y (2017) Effects of sea level rise and typhoon intensity on storm surge and waves in Pearl River estuary. Ocean Eng 136:80–93
Yuan S, Li L, Amini F, Tang H (2014) Numerical study of turbulence and erosion of an HPTRM strengthened levee under combined storm surge overflow and wave overtopping. J Coastal Res 30(1):142–157

Website visited

https://adcirc.org/products/adcirc-tidal-databases/
https://stn.wim.usgs.gov/FEV/
https://waterdata.usgs.gov/fl/nwis/uv?site_no=02359170
https://www.ndbc.noaa.gov/
https://www.nhc.noaa.gov/data/#hurdat
https://www.ndbc.noaa.gov/station_history.php?station=apcf1